

The Velocity Field from Type Ia Supernovae Matches the Gravity Field from Galaxy Surveys

Adam G. Riess¹, Marc Davis¹, Jonathan Baker¹ & Robert P. Kirshner²

¹Department of Astronomy, University of California, Berkeley, CA 94720-3411

²Harvard-Smithsonian Center for Astrophysics, 60 Garden Street, Cambridge, MA 02138

Received _____; accepted _____

ABSTRACT

We compare the peculiar velocities of nearby SNe Ia with those predicted by the gravity fields of full sky galaxy catalogs. The method provides a powerful test of the gravitational instability paradigm and strong constraints on the density parameter $\beta \equiv \Omega^{0.6}/b$. For 24 SNe Ia within 10,000 km s⁻¹, we find the observed SNe Ia peculiar velocities are well modeled by the predictions derived from the 1.2 Jy IRAS survey and the Optical Redshift Survey (ORS). Our best β is 0.4 from IRAS, and 0.3 from the ORS, with $\beta > 0.7$ and $\beta < 0.15$ ruled out at 95% confidence levels from the IRAS comparison. Bootstrap resampling tests show these results to be robust in the mean and in its error. The precision of this technique will improve as additional nearby SNe Ia are discovered and monitored.

subject headings: supernovae:general ; cosmology:observations, large-scale structure of universe—Local Group

1. Introduction

The motions of galaxies probe the size of potentials formed by the gravitating matter in the Universe. Redshift surveys map the spatial distribution of luminous matter. Together, the two measure the contribution of luminous and dark matter to the contents of the Universe, providing a direct measure of the density parameter on the largest possible scale.

Previous attempts to test the gravitational instability paradigm and constrain the mass density parameter, Ω_0 , are hindered by imprecise distance estimates to individual galaxies. Distance indicators based on empirical relationships between galaxy luminosity and internal velocity (i.e., Tully-Fisher and $D_n - \sigma$) yield individual distance uncertainties of 20-25% (Jacoby et al 1992, Tully & Fisher 1977, Dressler et al 1987, Willick et al 1996). To increase the utility of such data, workers have amassed it in great quantity. While this strategy diminishes the random component of error, imprecise distances give rise to more troublesome systematic errors including selection bias, Malmquist bias, and smoothing biases (Strauss and Willick 1995). The antidote for such biases depends on knowledge of the distance uncertainty, a controversial quantity (Willick 1995, Mathewson & Ford 1994, Federspiel, Sandage, & Tammann 1994, Giovanelli & Haynes 1996). The forced marriage of inhomogeneous catalogs could result in additional errors in the inferred velocity field. Despite these challenges, remarkable progress has been made in this field (Dekel 1994, Dekel, Bertschinger, & Faber 1990, Davis, Nusser, & Willick 1996, Hudson 1994, Shaya, Peebles, & Tully 1995, Nusser & Davis 1994).

Type Ia supernovae are well suited to provide an independent test of the gravitational instability paradigm and to constrain the mass density. Light curves from the Calán/Tololo Survey (Hamuy et al 1993, 1996) and the CfA survey (Riess 1996, Riess et al 1997) yield distances with 5-10% uncertainty over the redshift range $1000 \leq cz \leq 36000$ km s⁻¹. Although the sample of observed SNe Ia is relatively small, the depth and precision

of supernova distances provide some advantages. For the reduction of random errors, one SN Ia is worth ~ 10 Tully-Fisher or Dn- σ measurements. Systematic bias, which rises with the square of the distance uncertainty, is also ~ 10 times smaller for SNe Ia distances. Individual distance errors can be derived from SNe Ia light curves (Riess, Press, and Kirshner 1995a, 1996) which give meaningful measurements of the deviation from smooth Hubble flow. Combining the SNe Ia data with models of the predicted “peculiar velocities”, one can constrain the mass density traced by galaxy fluctuations while testing the gravitational instability model for structure formation.

2. Analysis

The direct comparison of observed peculiar velocities and mass density fluctuations is not trivial. The problem becomes tractable only by assuming that the large scale component of the flow is single-valued and irrotational. Since galaxy fluctuations on scales larger than $10h^{-1}$ Mpc are observed to be less than unity (Davis and Peebles 1983), these assumptions are reasonable. Furthermore, for such fluctuations at late times, linear perturbation theory is quite accurate, and the expected velocity field $\mathbf{v}_{\mathbf{p}}$ can be related to the peculiar gravity field \mathbf{g} (Peebles 1980) by

$$\mathbf{v}_{\mathbf{p}}(\mathbf{r}) = \left(\frac{2}{3\Omega_0^{0.4}H_0} \right) \mathbf{g}(\mathbf{r}) \quad . \quad (1)$$

This equation simply states that the observed peculiar velocity results from the gravitational acceleration acting over a Hubble time.

The gravity field $\mathbf{g}(\mathbf{r})$ may be inferred from the distribution of galaxies which are assumed to trace the matter field. It is common to assume an unknown but linear bias exists between galaxy fluctuations δ_G and matter fluctuations δ_ρ , by employing a bias parameter b , i.e. $\delta_G = b\delta_\rho$. This simplification, while not accurate on small scales or in

dense environments, should suffice on large scales. Using linear theory, one can constrain only a combination of Ω_0 and b , $\beta \equiv \Omega_0^{0.6}/b$. A variety of methods for estimating $\mathbf{g}(\mathbf{r})$ from galaxy surveys are reviewed by Strauss and Willick (1995). Here, we use the method of Nusser and Davis (1994), which can successfully repair the gravitational distortions in redshift space. However, this technique cannot properly treat regions with multivalued relations between velocity and distance, expected near clusters of galaxies. The minimum smoothing scale of the derived gravity field is 500 km s^{-1} , and this smoothing increases with distance in proportion to the mean interparticle spacing of the galaxy catalog. This increase is necessary to suppress artificial two-body acceleration (Strauss et al 1992).

For comparison to the SNe Ia peculiar velocities, we computed the gravity field from the 1.2 Jy flux limited IRAS redshift survey of galaxies (Fisher et al 1995). This catalog contains 6010 galaxies with median redshift of 6000 km s^{-1} and provides a useful measure of the density field out to $cz \approx 15,000 \text{ km s}^{-1}$. The IRAS catalog is known to underrepresent the elliptical-rich cores of clusters relative to optically catalogs. Thus it is of interest to use the ORS catalog of optically selected galaxies for an alternative calculation of the gravity field (Santiago et al 1995, Baker et al 1997). The ORS contains 8457 galaxies, supplemented by the 1.2 Jy IRAS survey in sky regions without optical coverage.

We measured the distances and their uncertainties for 25 SNe Ia within $10,000 \text{ km s}^{-1}$ using MLCS distance measurements (Riess, Press, and Kirshner 1996). The redshifts of the SNe Ia come from Hamuy et al (1996), Riess (1996), and Riess et al (1997). Because of the limitation of linear biasing and the risk of multivalued flows, we conservatively discarded one SN Ia, SN 1992G, due to its proximity to the Virgo Cluster. In the directions of the remaining SNe, we computed the expected distance-redshift relations based on the gravity fields of either the ORS or IRAS surveys, as a function of β . Figure 1 shows an example of these curves. We assume a redshift error of 200 km s^{-1} as an estimate of the small scale

component of the radial peculiar velocity not describeable by linear theory.

For each SN, we have the distance d_i (in km s⁻¹), a distance error δd_i (in km s⁻¹), a redshift z_i , and a “redshift error”, $\delta cz_i = 200$ km s⁻¹. From the gravity maps, we have the functions $z(j, \beta)$ and $d(j, \beta)$ along a set of points j towards each SN’s direction. We seek the minimum separation of each point from the predicted curves, in units of the standard deviations. That is, for the i th SN Ia, we compute a contribution to a χ^2 ,

$$\delta\chi(\beta)_i^2 = \min_j \left(\left(\frac{d_i - d(j, \beta)}{\delta d_i} \right)^2 + \left(\frac{z_i - z(j, \beta)}{\delta z_i} \right)^2 \right), \quad (2)$$

where the minimization is over the locus of points j which defines the curve $z(d, \beta)$ toward each SN. A goodness of fit is computed by summing over all the SNe,

$$\chi(\beta)^2 = \sum_i \delta\chi(\beta)_i^2 \quad , \quad (3)$$

with results shown at the top of Figure 2 for both the IRAS and ORS surveys.

For the IRAS survey, we find $\beta_{IRAS} = 0.40 \pm 0.15$ and for the ORS survey we find $\beta_{ORS} = 0.30 \pm 0.10$. In both cases the value of χ^2 at the minimum is within the expected tolerance, confirming gravitational instability as a valid model for the observed peculiar motions of SNe Ia. We find $\frac{\beta_{ORS}}{\beta_{IRAS}} = 0.75 \pm .38$, in good agreement with the relative biasing of 0.7 derived from the correlation functions of ORS and IRAS galaxies (Fisher et al 1994).

The predicted and observed peculiar velocity fields for the best values of β are shown in Figure 3 in the Local Group (LG) frame at the location of each of the 24 SNe Ia; these numbers are also listed in Table 1. Although the gravity predictions are derived independently from the observed peculiar velocities, the similarity of the two is remarkable. The leverage any single SN Ia measurement has in determining β depends on its location. Because the dominant feature of the flow is dipolar, SNe Ia along the axis of this dipole carry more weight than those whose radial motion is perpendicular to it. Although the

supernova data can be extended to greater depth, beyond 10,000 km s⁻¹, the sampling of the IRAS and optical surveys is inadequate to derive useful peculiar velocity predictions.

3. Tests of Robustness

To verify that our results are free from the vagaries of our supernova and galaxy samples, we performed bootstrap resampling tests on both data sets. This procedure tests the effects our choice of sample points and their uncertainties have on the estimates of β by drawing new samples of data from our best estimate of the underlying population: our sample (Press et al. 1992).

We first drew 200 sets of randomly chosen SNe Ia from the sample of 24 SNe Ia, drawing each object with a Poisson probability of expectation value of 1. We then subjected each set to our maximum likelihood estimator for β , using the gravity field of the IRAS catalog. As seen on the bottom of Figure 2, the distribution for β preferred by the individual SNe Ia agrees well with the single likelihood distribution estimated from our sample.

Similarly, we tested the robustness of the IRAS gravity field by generating 20 bootstrap resampled IRAS catalogs, as we did for the resampled SNe catalogs. For each resampled IRAS catalog, we generated full gravity fields for the range $0.1 \leq \beta \leq 1.2$. The resulting β values derived from the minimum χ^2 of the 24 SNe sample are also shown at the bottom of Figure 2. Again, this distribution is consistent with the constraints for β inferred from the χ^2 of the original datasets. Thus we believe the estimates in §2 are reasonable.

4. Discussion

Figure 3 demonstrates the remarkable consistency between the observed peculiar velocities of 24 SNe Ia and those predicted from the gravity fields of optical or IRAS galaxies using linear perturbation theory and the best value for β . The excellent χ^2 fits in Figure 2 confirm our simple model for the source of peculiar velocities while putting useful constraints on the mass density parameter, β .

The signals, seen in Figure 3, are largely dipole patterns revealing the motion of the LG relative to the SNe frame. They constrain the *shear* in the large scale velocity field induced by the gravity of galaxies within the sample’s 10,000 km s⁻¹ radius. The bulk of the CMB dipole signature does appear to have been generated within this radius. Velocity dipole patterns that match the gravitational dipole signature have been detected in several other surveys (e.g. Riess, Press, and Kirshner 1995b, da Costa et al 1996; Giovanelli et al 1996), but flows inconsistent with the predicted gravity field for all β values have also been reported (Lauer and Postman, 1992, 1994; Davis, Nusser, and Willick 1996).

A more sophisticated, normal mode comparison of the IRAS gravity field to the velocity field derived from a sample of 2900 Mark-III Tully-Fisher galaxies within a limiting redshift of 6000 km s⁻¹ shows inconsistencies for any value of β (Davis, Nusser, and Willick 1996). This same procedure applied to the SFI catalog yields consistent gravity and velocity fields with $\beta_{IRAS} = 0.6 \pm 0.1$. The POTENT reconstruction of the local density field from the Mark-III catalog recovers many observed features in the IRAS maps and estimates $\beta = 0.89 \pm 0.12$, but some inconsistencies persist (Sigad et al 1997, Dekel 1994). The failure to match the fields remains unexplained.

By limiting the analysis to a redshift of 3000 km s⁻¹, Willick et al (1996) successfully applied the VELMOD algorithm to compare the IRAS gravity field to a sample of 838 Tully-Fisher galaxies; a maximum likelihood analysis leads to $\beta = 0.49 \pm 0.07$, is consistent with our results for the IRAS gravity field. Similar low values of the density parameter

emerge from the least action method applied to the flow field with 3000 km s^{-1} (Shaya, Peebles, and Tully 1995). These procedures are distinct and do not all suffer from the same biases. Thus it is encouraging that they are leading to consistent (and perhaps reliable) results.

In Figure 3, the individual peculiar velocities in the SN map appear to be slightly larger than the velocities predicted at the same locations by the IRAS or ORS fields. We attribute this to measurement noise and velocity noise (small scale velocity flows) present in the SN data but not in the heavily smoothed IRAS or ORS velocity fields. Because of this noise, some SN velocity residuals do not match the sign (filling in Figure 3) of the IRAS predictions and/or the mode of the signs of the hemisphere in which they occur. But overall, the χ^2 minimization for the supernovae takes these sources of error properly into account and produces the best matched β for the data sets. Our determinations of β are not sensitive to our estimate of the velocity noise or SNe Ia errors, the latter limited by the small dispersion from smooth Hubble flow. As the distances for individual supernovae increase, the errors (in km s^{-1}) increase, while for the IRAS and ORS data sets the smoothing becomes stronger and the amplitude of point to point variations gets smaller. Although more distant SNe carry less weight, we find the objects within as well as beyond 5000 km s^{-1} give consistently low values for β . Nusser and Davis (1995) show how to avoid the effects of mismatched smoothing that appear here, but the present SN sample is too sparse to apply their methods.

MLCS distances are precise enough to characterize the peculiar velocity field in the direction of each supernova. Yet, during this application we found intrinsic uncertainties still limit the precision of relative SNe Ia distances to no better than 5%. Future investigations into SNe observables may improve the precision of these distances or our understanding of their limitations.

As the supernova data set grows, the precision of this comparison between gravity and velocity will improve, and the methods of analysis that have been used on the galaxy data sets will become appropriate. No tool for mapping the peculiar velocity field has a brighter future.

Acknowledgements

This work was supported by NSF grant AST95-28340 and NASA grant NAG 5-1360 at UCB, NSF grants AST95-28899 and AST96-17058 at Harvard University and by the Miller Institute for Basic Research in Science through a fellowship to A.G.R..

Table 1: Peculiar Velocity Data

<i>SN Ia</i>	<i>l</i>	<i>b</i>	<i>cz</i> (km s ⁻¹)	<i>cz - H₀d</i> (km s ⁻¹)	<i>σ_d</i> (km s ⁻¹)	IRAS <i>v</i> (β = 0.4)	ORS <i>v</i> (β = 0.3)
(1)	(2)	(3)	(4)	(5)	(6)	(7)	(8)
1995al	192.60	51.40	1493.	-466.	123.	-407.	-365.
1996X	310.20	35.70	1845.	-96.	149.	-81.	-204.
1995D	230.00	39.67	2000.	-258.	156.	-457.	-191.
1996Z	253.60	22.60	2014.	-427.	289.	-320.	-71.
1991M	30.39	45.90	2489.	15.	201.	-183.	-229.
1992K	306.28	16.31	2825.	-381.	345.	-18.	17.
1995E	141.97	30.27	3639.	175.	217.	21.	-368.
1991ag	342.56	-31.64	4150.	-131.	289.	176.	358.
1992al	347.30	-38.50	4355.	566.	245.	187.	373.
1994S	187.84	85.75	4539.	81.	283.	-129.	-167.
1995bd	187.10	-21.70	4808.	227.	329.	46.	193.
1993ae	144.62	-63.23	5521.	333.	409.	226.	139.
1992bo	261.88	-80.35	5662.	424.	369.	99.	327.
1992bc	245.70	-59.64	6053.	551.	355.	-59.	282.
1994M	291.69	63.03	6730.	-716.	564.	-407.	-29.
1995ak	169.70	-49.00	6887.	1063.	578.	252.	221.
1993H	318.20	30.30	6982.	263.	443.	-156.	62.
1992ag	312.50	38.40	7295.	-489.	984.	-272.	78.
1992P	295.62	73.11	7447.	-519.	539.	-408.	-108.
1994Q	99.60	65.00	8956.	-790.	648.	-12.	-632.
1996C	64.38	39.68	8872.	-535.	819.	137.	-477.
1993ah	25.90	-76.80	8974.	-53.	1012.	183.	277.
1990O	37.60	28.40	9247.	-1062.	749.	5.	-197.
1991U	311.82	36.21	9290.	180.	1357.	-260.	23.

References

- Baker, J., Davis, M., Strauss, M., Lahav, O., Santiago, B. X., 1997, in preparation
da Costa, L., Freudling, W., Wegner, G., Giovanelli, R., Haynes, M., & Salzer, J.
1996,Ap.J.L., 468, L5
- da Costa, L., et al, 1997, in preparation
- Davis, M. & Peebles, 1983, ApJ, 267, 465
- Davis, M., Nusser, A., and Willick, J. 1996, ApJ, 473, 22
- Dekel, A., 1994, ARA&A, 32, 371
- Dekel, A., Bertschinger, E. & Faber, S. M., 1990, ApJ, 364, 349
- Dressler, A., Faber, S. M., Burstein, D., Davies, R. L., Lynden-Bell, D., Terlevich, R. J. &
Wegner, G. 1987, ApJ, 313, L37
- Federspiel, M., Sandage, A. & Tamman, G. A., 1994, ApJ, 430, 29
- Fisher, K., Huchra, J. P., Strauss, M. A., Davis, M., Yahil, A., Schlegel, D., 1995, ApJS,
100, 69
- Fisher, K., Davis, M., Strauss, M. A., Yahil, A., Huchra, J. P., 1994, MNRAS, 266, 50
- Giovanelli, R., Haynes, M., Wegner, G., da Costa, L., Freudling, W., & Salzer, J. 1996,
ApJ, 464, L99
- Hamuy, M., Phillips, M. M., Suntzeff, N.B., Schommer, R. A., Maza, R.A., & Aviles, R.
1997, AJ, 112, 2048
- Hamuy, M., et al 1993, AJ, 106, 2392
- Hudson, M. J., 1994, MNRAS, 266, 468
- Jacoby, G., et al, 1992, PASP, 104, 599
- Lauer, T., & Postman, M. 1992, Ap.J.Lett., 400, L47
- Lauer, T., & Postman, M. 1994, Ap.J. 425, 418
- Mathewson, D. S. & Ford, V. L., 1994, ApJ, 434, L39
- Nusser, A. & Davis, M., 1994, ApJ, 421, L1

- Nusser, A. & Davis, M., 1995, MNRAS, 276, 1391
- Peebles, P.J.E. 1980, The Large Scale Structure of the Universe, Princeton U. Press.
- Press, W.H., Teukolsky, S.A., Vetterling, W.T. & Flannery, B.P. 1992, *Numerical Recipes*,
2nd ed. (Cambridge University Press)
- Riess, A.G., Press W.H., Kirshner, R.P., 1995a, ApJ, 438 L17
- Riess, A.G., Press W.H., Kirshner, R.P., 1995b, ApJ, 445, L91
- Riess, A.G., Press, W.H., & Kirshner, R.P. 1996, ApJ, 473, 88
- Riess, A.G., PhD thesis, 1996, Harvard University
- Riess, A. G., et al 1997, in preparation
- Santiago, B. X., et al, 1995, ApJ, 446, 457
- Sigad, Y., Dekel, A., Strauss, M., & Yahil, A. 1997, in preparation
- Shaya, E., Peebles, P., and Tully, B. 1995, Astrophysical Journal, 454, 15.
- Strauss, M., & Willick, J. 1995, Physics Reports, 261, 271
- Strauss, M. A., Yahil, A., Davis, M., Huchra, J. P.& Fisher, K. B., 1992, ApJ, 397, 395
- Tully, R. B. & Fisher, J. R., 1977, A&A, 54, 661
- Willick, J., Strauss, M., Dekel, A., & Kolatt, T. 1996, preprint astro-ph/9612240
- Willick, J. A., Courteau, Faber, S. M., Burstein, D. & Dekel, A., 1995, ApJ, 446, 12

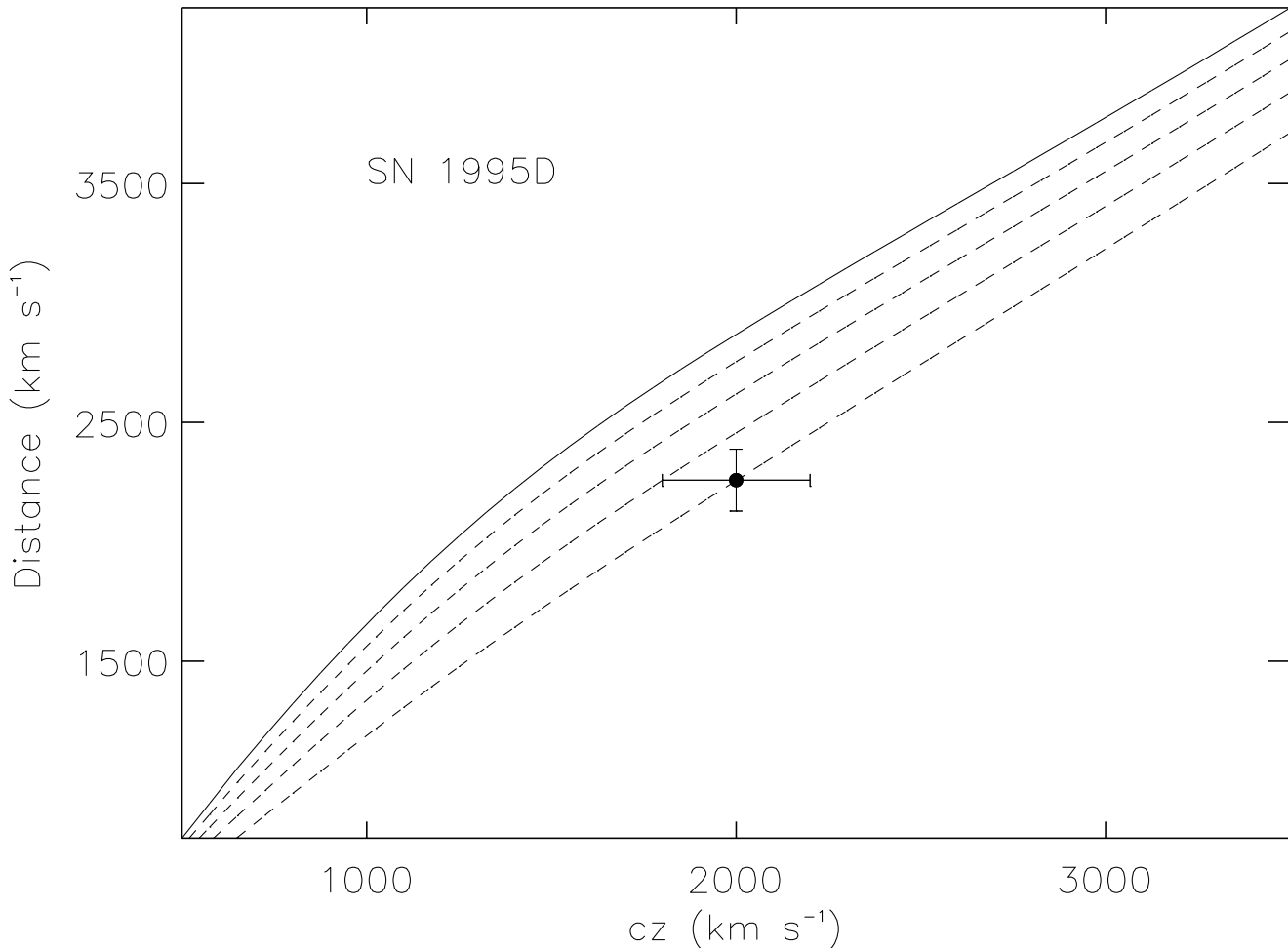


Fig. 1.— Velocity-distance relation in the vicinity of SNe Ia. This is an example of the velocity versus distance predictions of the IRAS gravity maps as a function of the mass density parameter, β , in the direction of SNe Ia. The solid line shows the $\beta = 1.0$ prediction, with subsequent dotted lines showing the predictions for β in decreasing increments of 0.2. Overplotted is the measurement of the SNe Ia redshift, MLCS distance (in km s⁻¹) and distance error with a small scale velocity error of 200 km s⁻¹. Such plots contributes to the determination of β via equation (2).

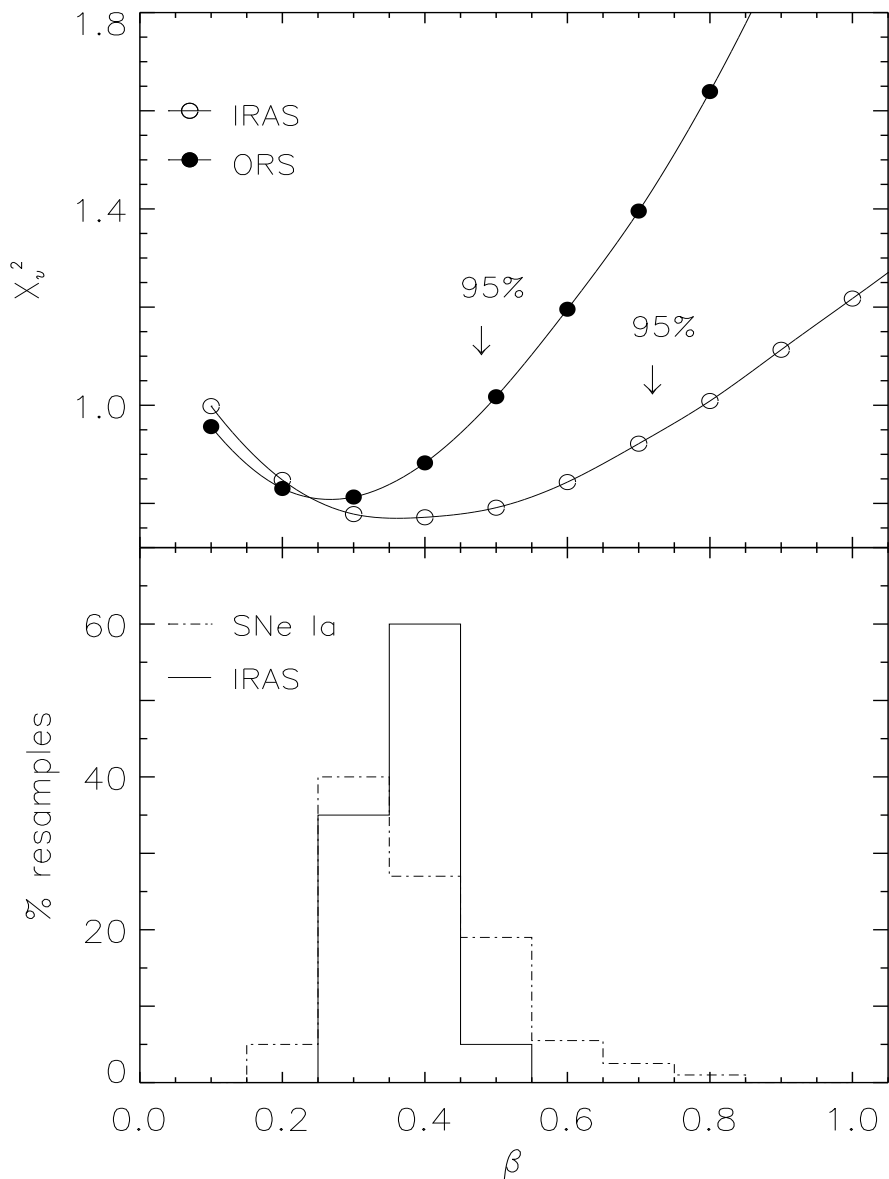


Fig. 2.— Constraints on the mass density parameter, β , and tests of robustness. The top panel shows the value of our χ^2 statistic as a function of β , equation (3), reduced (divided) by the twenty-three degrees of freedom. Our best β is 0.4 from IRAS, and 0.3 from the ORS, with $\beta > 0.7$ and $\beta < 0.15$ ruled out at 95% confidence levels for the comparison to IRAS. Bootstrap resamplings (bottom panel) of the SNe Ia and IRAS galaxies, described in §3, validate our estimates of β .

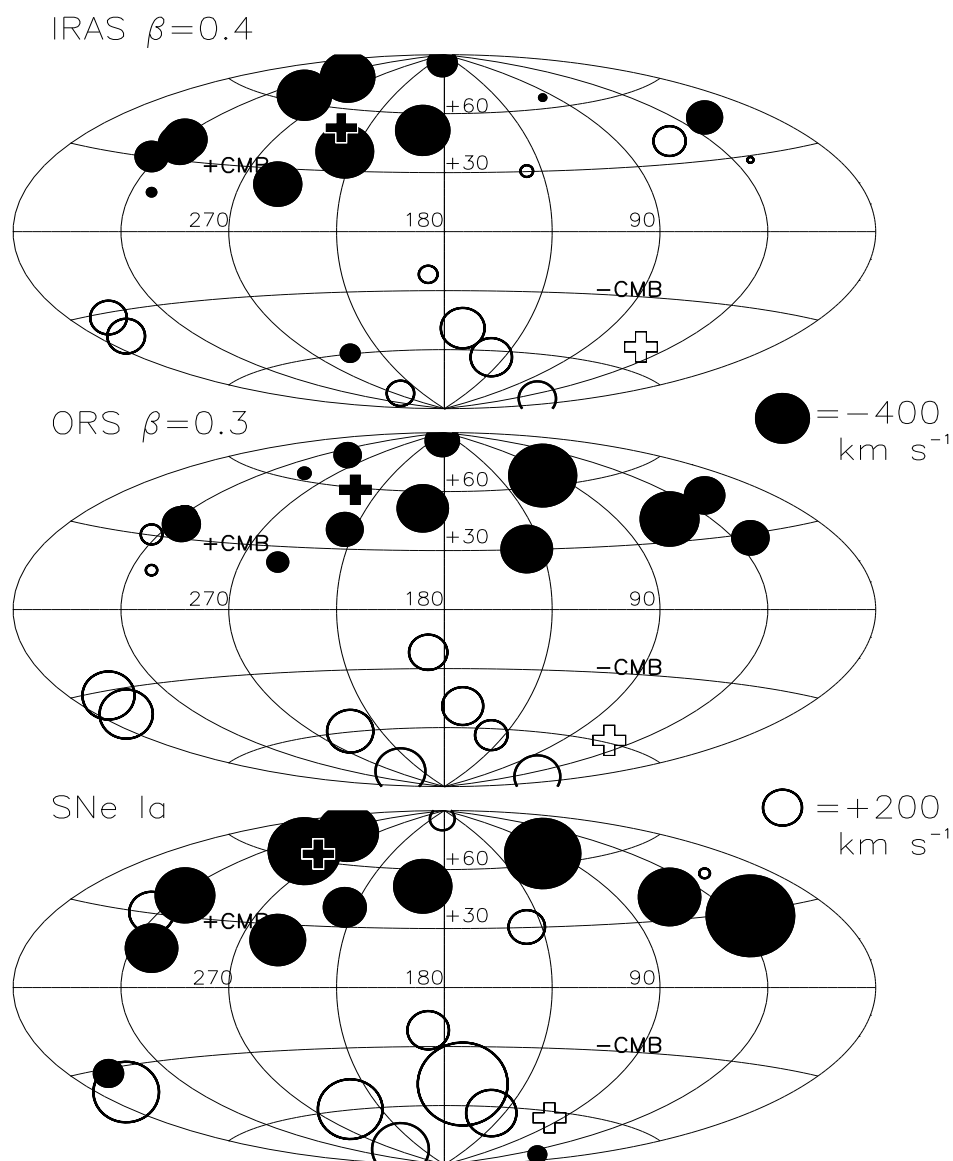


Fig. 3.— Predicted and observed peculiar velocity fields in the Local Group rest frame. Filled/Open points represent SNe Ia with measured negative/positive peculiar velocities (bottom map). The top two maps show the peculiar velocities predicted by the gravity fields of the IRAS and ORS catalogs at the position of the SNe Ia for values of β which best fit the SNe Ia velocity field. Filled/Open crosses mark the direction towards which the Local Group is approaching/receding. The directions of increased/decreased cosmic microwave background temperature are indicated by +CMB/-CMB.